Nanoscale determination of phase velocity by scanning acoustic force microscopy

E. Chilla,* T. Hesjedal, and H. -J. Fröhlich
Paul-Drude-Institute for Solid-State Electronics, Hausvogteiplatz 5-7, D-10117 Berlin, Germany
(Received 17 January 1997)

We measured the phase velocity of surface acoustic waves (SAW's) with a scanning acoustic force microscope (SAFM) and achieved a maximum lateral resolution of 19.9 nm. The phase measurement of high-frequency waves with a slowly responding SAFM cantilever was perfomed by frequency mixing at its nonlinear force curve. For Au layers of different thicknesses the SAW dispersion was studied on a lateral scale of 200 nm and compared to calculated data. [S0163-1829(97)03523-6]

I. INTRODUCTION

As the interest in nanostructures and in thin films has increased, so has the necessity for their mechanical characterization. The mechanical properties can notably alter as the size of the crystallites or the film thickness changes. Though it is well known that thin films often develop large intrinsic stresses during their preparation that can have an important impact on optic and electronic behavior and even affect structural self-organization, there is only poor knowledge about the elasticity on the nanometer scale.[1–3] The challenge of nanoelasticity studies is based on the fact that common methods, which have been used for the macroscopic investigation of the elastic properties of matter, can hardly be applied due to their limited lateral resolution. Well-established techniques that measure the phase velocity of propagating acoustic waves, like the line-focus acoustic microscope, are resolution limited to about one acoustic wavelength.[4] Therefore, even for frequencies up to the GHz range, acoustic phase delay determination by common methods are restricted to the micrometer scale and perform a lateral averaging over locally varying elastic properties that may be caused by nanostructures, surface stresses, or other material inhomogeneities. To this day the measurement of propagation velocities in the submicrometer range has not been reported.

The advent of local probe methods, particularly the atomic force microscope[5] has rapidly stimulated expectations for an elastic mapping with high lateral resolution. Much attention has recently been paid on studies of the behavior of the mechanical contact between the tip and the surface on a very small scale.[6,7] The idea of modulating the interaction force has been used for nanoindentation experiments to image surface elasticity with the atomic force microscope.[8] It is known that the inelastic deformation properties of small volumes are considerably different from bulk properties.[9] However, indentation experiments suffer from the rigid interaction between the probe and the sample. Hence, the quantitative elastic determination requires detailed knowledge about the interaction process as well as the mechanical properties of the tip and the cantilever.

Furthermore, near field acoustic microscopy, where Abbe's principle is no longer the limiting factor for the lateral resolution, has been discussed.[10] Various techniques based on scanning probe methods have been introduced inherently, offering a very local point of interaction.[11–13] The key of detecting acoustic waves by force microscopy is the shift of the cantilever's mean position due to high-frequency surface oscillations.[14] This shift is the static contribution due to self-mixing of the high-frequency modulation of the tip-to-sample distance by the nonlinear interaction force. It has also been used to detect vibrations at the surface of a bulk resonator.[15] Through the nonlinearity of the tunneling curve, the rf oscillation of a Au layer deposited on a piezoelectric crystal was also detected by a scanning tunneling microscope too.[16]

Recently, we mapped the lateral distribution of the surface oscillation amplitude by the scanning acoustic force microscope (SAFM) with a lateral resolution smaller than 1 μm,[17] opening a different way of the local study of damping phenomena. Contrary to these amplitude measurements, obtaining the phase of a rf wave needs a high-frequency detection system. However, the microscope's control unit as well as the cantilever's response is bandwidth limited. Therefore, the phase information has to be transfered to a detectable frequency range.

In this paper we report on the detection of the phase of surface oscillations within the nanometer scale based on nonlinear frequency mixing. We discuss the SAFM measurement of the phase velocity dispersion of surface acoustic waves (SAW's) that gives us the opportunity to determine the elastic properties within very small structures when solving the inverse problem of SAW propagation.[18]

II. EXPERIMENTAL DETAILS

In principle, the experimental setup consists of a SAW source with a SFM tip being positioned in the wave's propagation path. A second source is needed to launch the slightly frequency detuned probe waves. Then the mixing of the two waves takes place at the nonlinearity of the force curve. The sources generate SAW's in opposite directions so that the waves superimpose within the propagation path. Since the amplitude of the excited waves was only about 0.2 nm, nonlinear elastic effects for SAW propagation can be neglected.[19] The signal at the difference frequency is then analyzed by using a lock-in amplifier. In a first setup, the excitation of the SAW's was performed by interdigital transducers (IDT's), which generate plane waves with well-defined wave vectors $k=2\pi/\lambda$, where λ is the wavelength of the SAW. We have used splitfinger IDT's on ST-X quartz

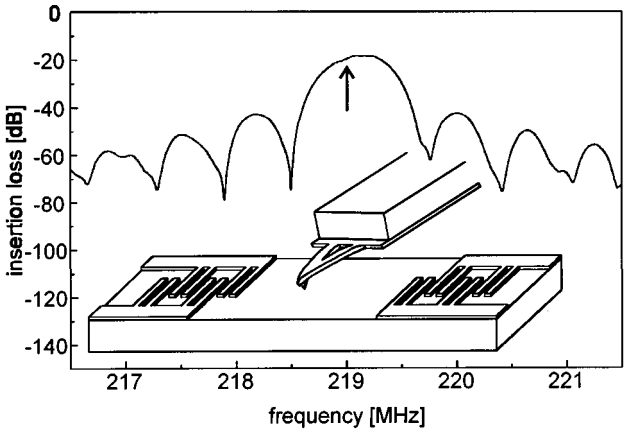

FIG. 1. Amplitude-frequency characteristic of the acoustic delay line formed by two interdigital transducers. The arrow marks the driving frequency. The inset shows the experimental setup.

(Euler angles: 0°, 132.75°, 0°) with the SAW propagation direction being parallel to the X crystal axis. In Fig. 1 the amplitude-frequency characteristic of the transmission between the two IDT's is displayed. We have excited the SAW's near the center frequency of the bandpass at 219 MHz. The inset to Fig. 1 shows the basic experimental setup. The IDT's are connected without electrical matching to rf generators with a power output lower than 10 dBm. The insertion loss of the delay line was 20 dB. The difference frequencies were lower than 100 kHz, which is as small as 0.05% of the operating frequency. The reference frequency for the lock-in amplifier, that detects the signal at the difference frequency, was generated by external mixing of the rf frequencies. When scanning the tip along the surface the electrical signal that is the reference clock for the acoustic

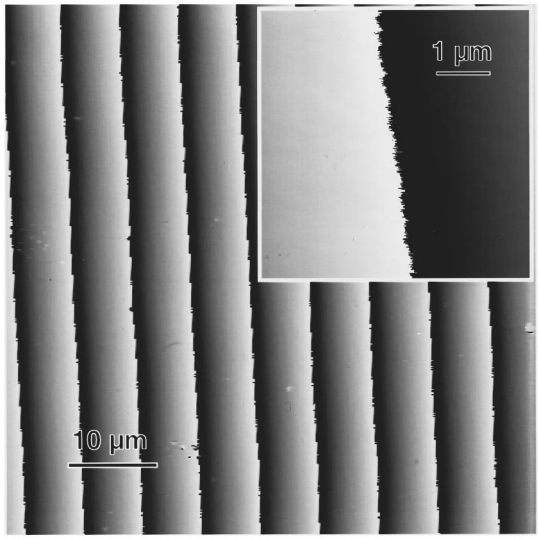

FIG. 2. SAFM measurement of the linear phase behavior of the plane waves excited by interdigital transducers. The phase jumps induced by the lock-in phase range of 360° have a separation of 6.83 μm. The inset zooms on such a phase jump demonstrating the stability of the phase measurement.

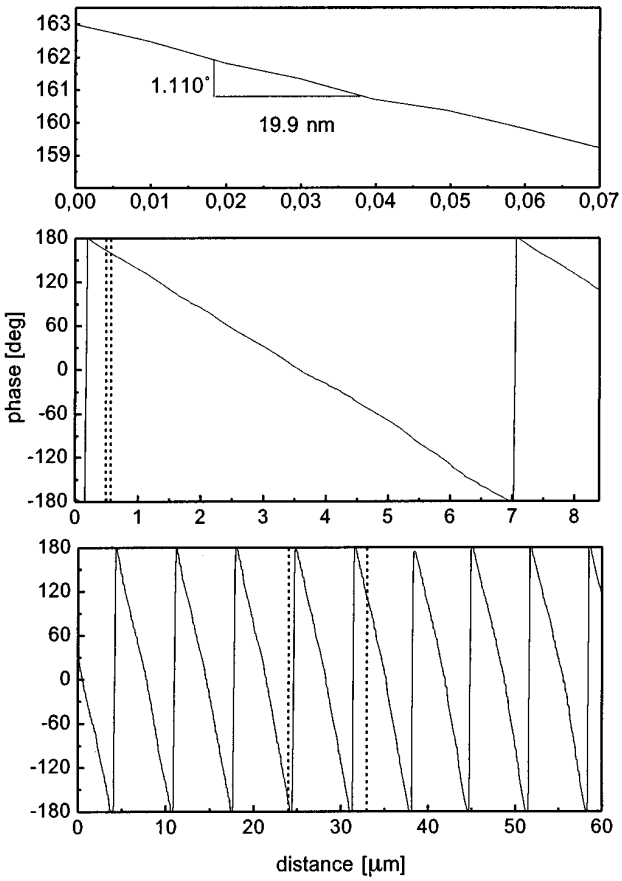

FIG. 3. Line scans of the linear phase dependence measured by the SAFM with the lower trace showing the 60 μm, the middle trace the 8.4 μm, and the upper trace the 70 nm measurement. The dotted lines mark the zooming in from the lower to the upper trace. For small scale scans the phase velocity is determined by the estimation of the phase slope. The maximum lateral resolution of the phase velocity determination was 19.9 nm.

measurement keeps constant while the phase of the surface oscillation changes due to the variation of the propagation length of the SAW's. The measured phase is determined by the delay of the SAW's at propagation length x. In detail, due to the contribution of two SAW's with the wavelengths λ_1 and λ_2, the phase change is $\varphi = 2\pi x(1/\lambda_1 + 1/\lambda_2) \approx 4\pi x/\lambda$, i.e., twice the phase delay of one SAW. The systematic error is the ratio of the difference frequency and the generator frequency. The utilizable difference frequencies range from 1 kHz to 100 kHz. However, higher frequencies are preferred allowing higher scan frequencies. We have performed 1 Hz and 0.2 Hz scans for preview and detailed images with 512 × 512 points per image, respectively. When choosing the lock-in time constant to 10 ms the lateral resolution of the phase measurements decreases with respect to the topographical image by only a factor of 2. Hence for 60 μm and 5.1 μm scans the phase resolution is limited by the software given step size to about 240 nm and 20 nm, respectively.

III. MEASUREMENTS AND DISCUSSION

Figure 2 shows a 60×60 μm^2 grayscale image of the

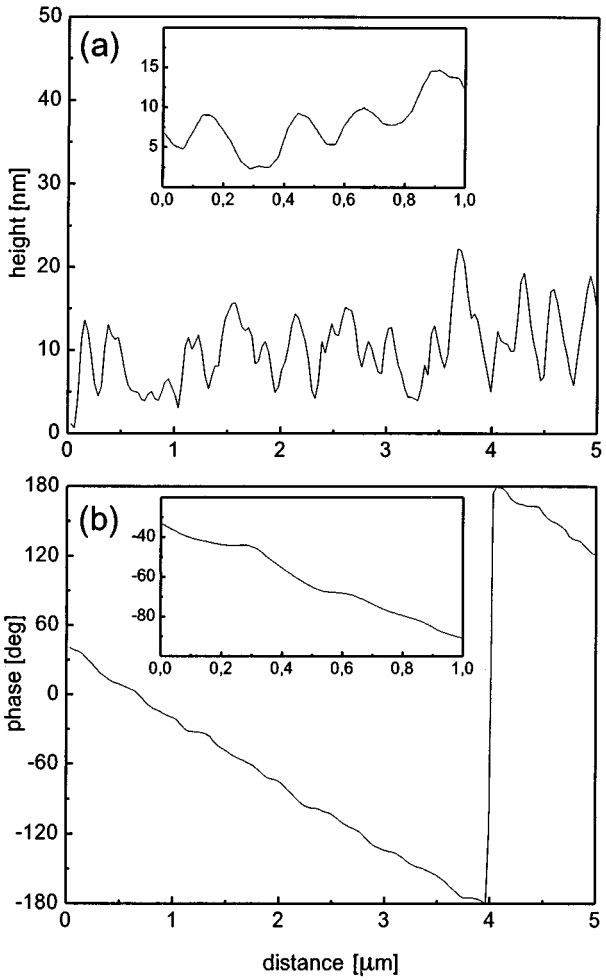

FIG. 4. SAFM measurement of (a) topography and (b) phase of a rough Au layer. The insets show the influence of the topographical gradients on the phase measurement.

linear phase delay for a Au layer of 93 ± 4 nm thickness. The direction of the wave vector is slightly rotated with respect to the scan direction. The 2π phase shifts are $\lambda/2$ separated. The scanner resolution limitation can be clearly observed at the wave front where a dither appears. The inset in Fig. 2 shows 5.1×5.1 μm^2 zoom of a phase shift. The stability of the phase measurement reaches almost the pixel resolution.

A. Phase velocity

When evaluating the wavelength over a range of five 2π phase shifts, a phase velocity $v = 2989 \pm 10.3$ m/s was obtained. Figure 3 shows the linear phase delay starting from 60 μm (lower trace), zooming to 8.4 μm (middle trace), and to 70 nm (upper trace). The span of the two zooms is marked by the dotted lines. Though the phase velocity is defined by the phase variation with respect to the propagation length the velocities can be measured on scales much smaller than the SAW wavelength. For a lateral distance of $\Delta x = 19.9$ nm the phase variation $\Delta\varphi = 1.110°$ was determined leading to a SAW phase velocity of 2827m/s. Compared with 2989 m/s obtained for the 60 μm scan, the deviation is only about 5.4%. However, the small scale velocity determination is

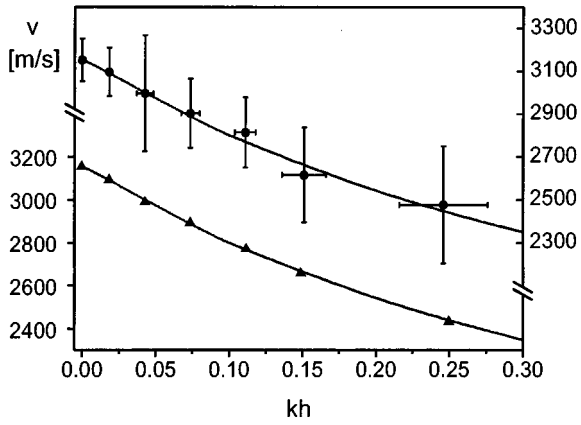

FIG. 5. SAW phase velocity dispersion $v(kh)$ of Au covered ST-X quartz with k being the wave vector and h the Au layer thickness. The velocity was measured for seven values of kh over a lateral distance of (○) 200 nm and (△) 10 π phase delay (28.3 – 36.0 μm). The solid lines represent the calculated dispersion curve.

very sensitive to topographical effects. The variation gradient of the phase delay enlarges with increasing corrugation. Figure 4(a) shows a 5 μm linescan of the topography of a rough Au layer and Fig. 4(b) shows the related phase delay. Even though the main phase behavior remains on a scale comparable to the grain size, large deviations from the linear phase delay appear. An 1 μm scan shows that these phase deviations [inset Fig. 4(b)] correlate with the surface topography [inset Fig 4(a)]. When measuring in areas with a large topographical height variation and a comparably small phase change there is a remarkable influence of the gradient of the topography on the phase. In this case not only a normal component of the force bends the lever but there are also lateral components. Those can be explained by the assumption that at grain boundaries the interaction area of the pyramidally shaped tip with the corrugated surface extends and that the local friction increases. This effect of undesired lever bending and twisting must be carefully separated from the contribution of the real local elastic properties of the surface. A possible way of obtaining the real phase delay is the averaging over several neighboring linescans.

B. Dispersion

Figure 5 shows the SAFM measurement of the SAW phase velocity dispersion. To obtain a wide range of thickness dependence a series of samples with different Au thicknesses h was processed. The lower part of Fig. 5 displays the velocity measurement for a phase delay of 10 π, i.e., a propagation path between 36.0 and 28.3 μm depending on the SAW wavelength. The measurement errors of about 0.3% are mainly limited by the scanner resolution of 512 points/line. The solid line describes the calculated values for the SAW. The calculation has been provided by the transfer matrix method using the standard material constants.[20] The upper part displays the velocity determined by a phase slope measurement on a lateral scale of 200 nm. As the wavelength determination is strongly affected by the roughness of the topography, large errors for the wave number as well as for the velocity occur. The influence of the topography was re-

duced by averaging over ten parallel scans. The solid circles in the upper part of Fig. 5 represent the mean values.

IV. CONCLUSION

We have reported measurements of the phase velocity of acoustic waves on the nanometer scale by the SAFM. A maximum lateral resolution of 19.9 nm was reached. For high resolution phase velocity determination the roughness of the topography has a large influence on the accuracy of the wavelength determination. In contrast to other local elastic probing techniques, SAFM has the advantage of reducing this influence by topographical averaging. We have used the SAFM to study the SAW dispersion of a thin Au layer on a lateral scale of 200 nm. The measurement of the phase velocity dispersion on the nanometer scale opens the possibility for the exact determination of elastic constants of strained surfaces, quantum dots and wires, as well as the prediction of stress relaxation and surface reconstruction by a method that zooms the knowledge of well-known integral properties of layers down to small objects.

*Electronic address: e.chilla@pdi.wias-berlin.de

[1] S. C. Jain, M. Willander, and H. Maes, Semicond. Sci. Technol. **11**, 641 (1996).

[2] J. -Y. Marzin, J. -M. Gérard, A. Izraël, D. Barrier, and G. Bastard, Phys. Rev. Lett. **73**, 716 (1994).

[3] P. V. Santos, A. Cantarero, M. Cardona, R. Nötzel, and K. Ploog, Phys. Rev. B **52**, 1970 (1995).

[4] J. D. Achenbach, J. O. Kim, and Y. -C. Lee, in *Advances in Acoustic Microscopy*, edited by G. A. D. Briggs (Plenum Press, New York, 1995), Vol. 1, p. 153.

[5] G. Binnig, C. F. Quate, and Ch. Gerber, Phys. Rev. Lett. **56**, 930 (1986).

[6] N. A. Burnham, A. J. Kulik, G. Gremaud, and G. A. D. Briggs, Phys. Rev. Lett. **74**, 5092 (1995).

[7] N. Agrait, G. Rubio, and S. Viera, Phys. Rev. Lett. **74**, 3995 (1995).

[8] P. Maivald, H. J. Butt, S. A. C. Gould, C. B. Prater, B. Drake, J. A. Gutley, V. B. Ellings, and P. K. Hansma, Nanotechnology **2**, 103 (1991).

[9] S. P. Jarvis, A. Oral, T. P. Weihs, and J. B. Pethica, Rev. Sci. Instrum. **64**, 3515 (1993).

[10] B. T. Khuri-Yakub, S. Akamine, S. Hadimioglu, S. Yamada, and C. F. Quate, SPIE: Proc. **1556**, 30 (1991).

[11] K. Takata, T. Hasegawa, S. Hosaka, S. Hosoki, and T. Komoda, Appl. Phys. Lett. **55**, 1718 (1989).

[12] B. Cretin and F. Stahl, Appl. Phys. Lett. **62**, 829 (1993).

[13] U. Rabe and W. Arnold, Appl. Phys. Lett. **64**, 1493 (1994).

[14] W. Rohrbeck and E. Chilla, Phys. Status Solidi A **131**, 69 (1992).

[15] O. Kolosov and K. Yamanaka, Jpn. J. Appl. Phys. **32**, L1095 (1993); K. Yamanaka, K. Ogiso, and O. Kolosov, *ibid.* **33**, 3197 (1994); Appl. Phys. Lett. **64**, 178 (1994).

[16] W. Rohrbeck, E. Chilla, H. -J. Fröhlich, and J. Riedel, Appl. Phys. A **52**, 344 (1991); E. Chilla, W. Rohrbeck, H. -J. Fröhlich, R. Koch, and K. H. Rieder, Appl. Phys. Lett. **61**, 3107 (1992); Ann. Phys. (Leipzig) **3**, 21 (1994); T. Hesjedal, E. Chilla, and H. -J. Fröhlich, Appl. Phys. Lett. **69**, 354 (1996).

[17] T. Hesjedal, E. Chilla, and H. -J. Fröhlich, Appl. Phys. A **61**, 237 (1995).

[18] S. Makarov, E. Chilla, and H. -J. Fröhlich, J. Appl. Phys. **78**, 5028 (1995).

[19] Assuming that both IDT's contribute with 10 dBm each to the delay line losses, the amplitude is given after G.W. Farnell, Wave Electron. **2**, 1 (1976) by $u=4.2\times10^{-6}(W/\omega)^{1/2}$ $(\mathrm{m}^3/\mathrm{W\ s})^{1/2}$, with $W=(1\ \mathrm{mW}/330\ \mu\mathrm{m})$ being the acoustic beam power per meter of aperture and $\omega/2\pi=219$ MHz the SAW frequency. Nonlinear effects of wave propagation were found by W. Gibson *et al.*, J. Appl. Phys. **45**, 3288 (1974), to appear on ST-X quartz at amplitudes above 1 nm.

[20] A. J. Slobodnik, E. D. Conway, and R. T. Delmonico, *Microwave Acoustic Handbook* (NTIS, Springfield, Virginia, 1973), Vol. 1; G. Kovacs, M. Ahorn, H. E. Engan, G. Visintini, and C. C. W. Ruppel, in *Proceedings IEEE Ultrasonics Symposium*, Honolulu, 1990, edited by B. R. MvAvoy (IEEE, New York, 1990), p. 435.